J|A|C|S COMMUNICATIONS

Published on Web 11/24/2010

Pt-Decorated PdCo@Pd/C Core−Shell Nanoparticles with Enhanced Stability and Electrocatalytic Activity for the Oxygen Reduction Reaction

Deli Wang,[†] Huolin L. Xin,[†] Yingchao Yu,[†] Hongsen Wang,[†] Eric Rus,[†] David A. Muller,[‡,§] and Hector D. Abruña*[,†]

Department of Chemistry and Chemical Biology and Department of Physics, School of Applied and Engineering Physics, and Kavli Institute at Cornell for Nanoscale Science, Cornell University, Ithaca, New York 14853, United States

Received September 1, 2010; E-mail: hda1@cornell.edu

Abstract: A simple method for the preparation of PdCo@Pd core−shell nanoparticles supported on carbon based on an adsorbate-induced surface segregation effect has been developed. The stability of these PdCo@Pd nanoparticles and their electrocatalytic activity for the oxygen reduction reaction (ORR) were enhanced by decoration with a small amount of Pt deposited via a spontaneous displacement reaction. The facile method described herein is suitable for large-scale, lower-cost production and significantly lowers the Pt loading and thus the cost. The as-prepared PdCo@Pd and Pd-decorated PdCo@Pd nanocatalysts have a higher methanol tolerance than Pt/C in the ORR and are promising cathode catalysts for fuel cell applications.

The high cost and scarcity of Pt pose serious problems for the widespread commercialization of fuel cell technologies.[1] Recently, Pd-based cathode catalysts have attracted much attention because Pd possesses properties similar to those of Pt (same group of the periodic table, same crystal structure, and similar atomic size). The cost of Pd, however, is currently about one-third that of Pt, and it is at least 50 times more abundant than Pt.[2] Although Pd catalysts exhibit some catalytic activity toward the oxygen reduction reaction (ORR), especially with the incorporation of other metallic elements[1c,3] and even when decorated with heteropolyacids,[4] insufficient electrocatalytic activity and stability still remain as major obstacles for fuel cell applications. While the bimetallic Pt−Pd system could act as an alternative means of improving the ORR activity of Pd catalysts,[1a,5] this kind of catalyst still requires a relatively high Pt loading.

Herein, we describe a simple method of preparing PdCo@Pd core−shell nanoparticles on carbon by post-treatment of the as-prepared PdCo/C catalysts at high temperature under flowing H_2. To increase the open-circuit potential of the PdCo@Pd core−shell nanocatalysts for the ORR, the PdCo@Pd nanoparticles are decorated with a very small amount of Pt deposited via a spontaneous displacement reaction. Previously, nanoparticles with a Pt monolayer have been prepared by first laying down a Cu monolayer via underpotential deposition (UPD)[6] and then replacing Cu with a Pt monolayer by galvanic displacement. The amount of electrocatalyst that can be synthesized by this method is limited because the nanoparticles must be immobilized on a glassy carbon electrode to carry out the Cu UPD. The facile method described herein is suitable for large-scale, low-cost production and significantly lowers the Pt loading relative to other bimetallic Pt−Pd systems.

The carbon-supported PdCo@Pd core−shell nanoparticles were prepared via a two-step route (Figure S1 in the Supporting Information). First, $PdCl_2$ and $CoCl_2$ precursors that had been preadsorbed on the carbon were simultaneously reduced under flowing H_2 in a tube furnace.[7] The as-prepared PdCo/C catalysts were then annealed at 500 °C under flowing H_2 to yield particles with a core−shell structure. This procedure is based on the adsorbate-induced surface segregation effect.[8] According to the literature, the surface composition of a bimetallic system can be very different from the bulk composition, depending on the heat of segregation and the surface mixing energy.[9] In addition, differences in the gas adsorption energy on two metals can also induce surface segregation.[10] In our case, when annealed at high temperatures, the PdCo/C alloys undergo phase segregation in which the Pd migrates to the surface, forming a pure Pd overlayer on the bulk alloy, since the adsorption enthalpy of H on Pd is higher than that on Co.[11] The deposition of Pt on the PdCo@Pd surface was spontaneous because the equilibrium electrode potential of the $PtCl_4^{2-}$/Pt couple [0.775 V vs a standard hydrogen electrode (SHE)] is more positive than those of the $PdCl_4^{2-}$/Pd (0.591 V vs SHE) and Co^{2+}/Co (−0.28 V vs SHE) couples. Although the potential difference between the $PtCl_4^{2-}$/Pt and Co^{2+}/Co couples is much larger than that between the $PtCl_4^{2-}$/Pt and $PdCl_4^{2-}$/Pd couples, the Pt may primarily be deposited by displacement of Pd since the catalyst surface is Pd-rich after anealing and prior to Pt deposition (Figure S1). To verify that Pt spontaneously displaced Pd, we substituted the Pd/C catalyst for the core−shell PdCo@Pd/C catalyst and repeated the same procedure. The cyclic voltammogram (CV) and CO-stripping behavior of the Pd/C catalyst were different after the Pt deposition procedure, suggesting that Pt was indeed deposited on the Pd/C catalysts (Figure S2).

The core−shell structure and chemical distribution of PdCo@Pd/C nanoparticles were examined using an aberration-corrected 100 keV Nion scanning transmission electron microscope (STEM) equipped with an Enfina electron energy loss spectrometer (EELS) in which the electron beam is focused down to a 0.1−0.14 nm spot and scanned to form compositional maps.[12] Figure 1a,b shows a pair of annular dark-field (ADF)- and bright-field (BF)-STEM images simultaneously acquired prior to EELS map acquisition. These images reveal the internal crystal structure of the nanoparticle. Figure 1c,d shows the projected Co and Pd distributions within the particle extracted from a 146 × 127 pixel spectroscopic image. The Pd (red) vs Co (green) composite image (Figure 1e) demonstrates that a Pd-rich shell was formed on the surfaces. On the basis of a comparison of the line profiles across the Pd-rich shell from the Co and Pd maps (Figure 1f), the thickness of the shell was estimated to be ∼1 nm. A comparison of ADF-STEM images of PdCo@Pd/C and Pt-decorated PdCo@Pd/C nanoparticles is shown

[†] Department of Chemistry and Chemical Biology and Department of Physics.
[‡] School of Applied and Engineering Physics.
[§] Kavli Institute at Cornell for Nanoscale Science.

 10.1021/ja107874u

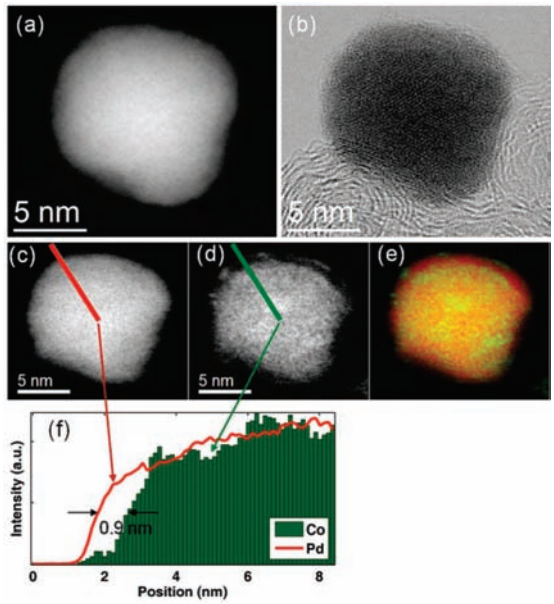

Figure 1. (a) ADF- and (b) BF-STEM images of a PdCo@Pd core−shell nanoparticle; EELS maps of (c) Pd and (d) Co along with (e) an overlay of those two maps; and (f) EELS line profiles of Pd and Co showing the Pd shell.

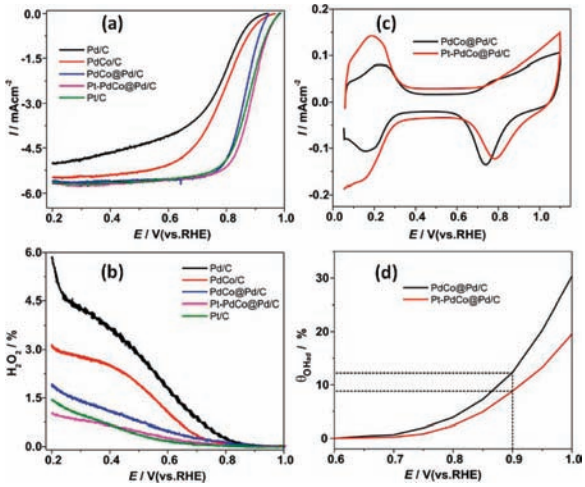

Figure 2. (a) ORR polarization curves. (b) Peroxide generation from the ORR detected at the ring electrode in O_2-saturated 0.1 M $HClO_4$. Sweep rate, 5 mV s^{-1}; rotation rate, 1600 rpm; ring potential, 1.2 V vs RHE. (c) CVs of different catalysts in 0.1 M $HClO_4$ purged with N_2. (d) Potential dependence of hydroxyl surface coverage (θ_{OH}).

in Figure S3. There is no appreciable distinction except a slight contrast difference between the two images.

Structural characterization of the as-prepared catalysts was carried out using X-ray diffraction (XRD) (Figure S4). All of the samples showed a typical face-centered-cubic pattern. After heat treatment, the diffraction peaks of PdCo/C shifted to higher angles relative to those of Pd/C, indicating a lattice contraction due to the alloying of Pd with Co. There was essentially no difference after Pt deposition because the amount of Pt was too small to be detected using XRD. However, the presence of Pt was verified by X-ray photoelectron spectroscopy (XPS) (Figure S5).

Figure 2 shows the polarization curves of the ORR for different catalysts (Figure 2a) and the corresponding hydrogen peroxide production measured using a rotating ring−disk electrode in which the glassy carbon disk was modified with the catalyst and the Pt

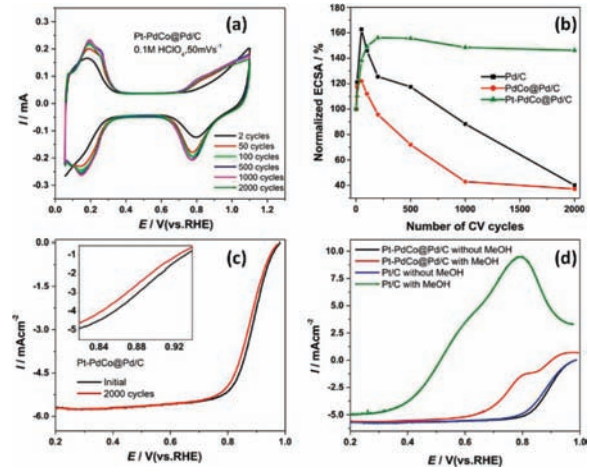

Figure 3. (a) CVs of the Pt-decorated PdCo@Pd/C catalyst after various numbers of potential cycles. (b) ECSA as a function of the number of CV cycles for different catalysts in N_2-purged 0.1 M $HClO_4$ solution. (c) ORR polarization curves for the Pt-decorated PdCo@Pd/C catalyst before and after cycling. (d) Polarization curves for the Pt−PdCo@Pd/C and Pt/C catalysts in O_2-saturated 0.1 M $HClO_4$ in the presence of 1 M MeOH. Rotation rate, 1600 rpm; sweep rate, 5 mV s^{-1}.

ring was used to detect the generated peroxide (Figure 2b). All of the electrodes were pretreated by cycling the potential between 0.05 and 1.1 V at a sweep rate of 50 mV s^{-1} for 50 cycles in order to remove any surface contamination prior to ORR activity testing. The rate of the ORR was significantly enhanced by PdCo/C and especially by PdCo@Pd/C relative to Pd/C. The amounts of peroxide detected at the ring electrode were diminished relative to Pd/C. The CVs of PdCo@Pd/C and Pt−PdCo@Pd/C are shown in Figure 2c. The currents were normalized to the metal surface area, which was estimated from the coulometric charge of the oxide reduction peak. For Pt−PdCo@Pd/C, the potentials of surface oxide formation and reduction were both more positive than those of PdCo@Pd/C, suggesting fast hydroxyl adsorption/desorption from the Pt−PdCo@Pd/C surfaces at more positive potentials. Decoration with Pt modified the ability of the catalyst to adsorb hydroxyl species (OH_{ad}). The Pt-decorated PdCo@Pd/C catalyst clearly had a lower OH coverage than PdCo@Pd/C over the entire potential range (Figure 2d). Since adsorbed OH species inhibit the ORR, the lower OH_{ad} coverage on the surface of the Pt−PdCo@Pd/C catalysts improves the ORR kinetics. Furthermore, modification of the electronic structure could also affect the catalytic behavior of the materials. The electronic structure of Pt deposited on the PdCo@Pd/C surfaces is different from that of bulk Pt because of the so-called strain and ligand effects of the core substrate.[13]

Degradation of the catalysts was evaluated by cycling the electrode potential between 0.05 and 1.1 V versus a reversible hydrogen electrode (RHE). Figure 3a shows the CVs of the Pt-decorated PdCo@Pd/C catalyst after an increasing number of potential cycles. For comparison, the CVs of Pd/C and PdCo@Pd/C catalysts are shown in Figure S6. The electrochemical surface area (ECSA, obtained from the integrated coulometric charge of the oxide reduction peaks) as a function of the number of potential cycles for each of the catalysts is shown in Figure 3b. It can be seen that each catalyst shows an increased ECSA in the first few cycles, which could be attributed to surface roughening and removal of contaminants from the sample surface. However, the ECSA of Pd/C and PdCo@Pd/C catalysts decreased substantially after 50 cycles, indicating their instability. In contrast, the ECSA of the Pt-decorated PdCo@Pd/C catalyst decreased only slightly after 2000 cycles, indicating that the PdCo@Pd/C catalyst was

stabilized by the Pt adlayer. The Pt−PdCo@Pd/C catalyst exhibited a degradation of only 10 mV in the half-wave potential for the ORR after having been cycled 2000 times (Figure 3c). The methanol tolerance of the catalysts for ORR was tested in O_2-saturated 0.1 M $HClO_4$ in the presence of 1 M methanol. As shown in Figure 3d, for Pt/C, the current transitioned from negative to positive at approximately +0.5 V in the presence of methanol, and there was a large current peak at +0.8 V. The observed behavior was caused by the competition between methanol oxidation and oxygen reduction, in which the ORR current was overwhelmed by the methanol oxidation current. However, the ORR activity of the Pt-decorated PdCo@Pd/C catalyst was much less affected in the presence of methanol, pointing to the potential use of this catalyst in direct methanol fuel cells.

In conclusion, PdCo@Pd/C core−shell nanoparticles were successfully synthesized using an H_2-induced surface segregation effect. An ultralow loading of Pt was deposited on the surface of the PdCo@Pd/C nanoparticles by a spontaneous displacement reaction, and the Pt-decorated PdCo@Pd/C catalyst was found to have significantly enhanced stability and ORR activity. The core−shell PdCo@Pd/C catalyst and the Pt-decorated PdCo@Pd/C catalyst showed much higher MeOH tolerances than Pt/C. The simple synthesis method and the significantly lower cost of the Pt−PdCo@Pd/C catalyst could enhance the commercial viability of fuel cell technologies.

Acknowledgment. This work was supported by the Department of Energy though Grant DE-FG02-87ER45298 by the Energy Materials Center at Cornell, an Energy Frontier Research Center funded by the U.S. Department of Energy, Office of Science, Office of Basic Energy Sciences, under Award DE-SC0001086. This work made use of the TEM and XPS facilities at the Cornell Center for Materials Research (CCMR).

Supporting Information Available: Synthesis, physical characterization, and electrochemical stability test details. This material is available free of charge via the Internet at http://pubs.acs.org.

References

(1) (a) Lim, B.; Jiang, M. J.; Camargo, P. H. C.; Cho, E. C.; Tao, J.; Lu, X. M.; Zhu, Y. M.; Xia, Y. A. *Science* **2009**, *324*, 1302. (b) Stamenkovic, V. R.; Mun, B. S.; Arenz, M.; Mayrhofer, K. J. J.; Lucas, C. A.; Wang, G. F.; Ross, P. N.; Markovic, N. M. *Nat. Mater.* **2007**, *6*, 241. (c) Fernandez, J. L.; Raghuveer, V.; Manthiram, A.; Bard, A. J. *J. Am. Chem. Soc.* **2005**, *127*, 13100.

(2) Antolini, E. *Energy Environ. Sci.* **2009**, *2*, 915.

(3) (a) Savadogo, O.; Lee, K.; Oishi, K.; Mitsushima, S.; Kamiya, N.; Ota, K. I. *Electrochem. Commun.* **2004**, *6*, 105. (b) Yeh, Y. C.; Chen, H. M.; Liu, R. S.; Asakura, K.; Lo, M. Y.; Peng, Y. M.; Chan, T. S.; Lee, J. F. *Chem. Mater.* **2009**, *21*, 4030. (d) Suo, Y. G.; Zhuang, L.; Lu, J. T. *Angew. Chem., Int. Ed.* **2007**, *46*, 2862.

(4) Wang, D. L.; Lu, S. F.; Jiang, S. *Chem. Commun.* **2010**, *46*, 2058.

(5) (a) Peng, Z. M.; Yang, H. *J. Am. Chem. Soc.* **2009**, *131*, 7542. (b) Chen, Z. W.; Waje, M.; Li, W. Z.; Yan, Y. S. *Angew. Chem., Int. Ed.* **2007**, *46*, 4060.

(6) (a) Wang, J. X.; Inada, H.; Wu, L. J.; Zhu, Y. M.; Choi, Y. M.; Liu, P.; Zhou, W. P.; Adzic, R. R. *J. Am. Chem. Soc.* **2009**, *131*, 17298. (b) Zhou, W. P.; Yang, X. F.; Vukmirovic, M. B.; Koel, B. E.; Jiao, J.; Peng, G. W.; Mavrikakis, M.; Adzic, R. R. *J. Am. Chem. Soc.* **2009**, *131*, 12755.

(7) (a) Wang, D. L.; Lu, S. F.; Jiang, S. P. *Electrochim. Acta* **2010**, *55*, 2964. (b) Wang, D. L.; Zhuang, L.; Lu, J. T. *J. Phys. Chem. C* **2007**, *111*, 16416.

(8) Mayrhofer, K. J. J.; Juhart, V.; Hartl, K.; Hanzlik, M.; Arenz, M. *Angew. Chem., Int. Ed.* **2009**, *48*, 3529.

(9) (a) Ruban, A. V.; Skriver, H. L.; Nørskov, J. K. *Phys. Rev. B* **1999**, *59*, 15900. (b) Christensen, A.; Ruban, A. V.; Stoltze, P.; Jacobsen, K. W.; Skriver, H. L.; Nørskov, J. K.; Besenbacher, F. *Phys. Rev. B* **1997**, *56*, 5822.

(10) (a) Yin, Y.; Rioux, R. M.; Erdonmez, C. K.; Hughes, S.; Somorjai, G. A.; Alivisatos, A. P. *Science* **2004**, *304*, 711. (b) Nerlov, J.; Chorkendorff, I. *Catal. Lett.* **1998**, *54*, 171.

(11) Popova, N. M.; Babenkova, L. V. *React. Kinet. Catal. Lett.* **1979**, *11*, 187.

(12) Muller, D.; Fitting Kourkoutis, L.; Murfitt, M.; Song, J. H.; Hwang, H. Y.; Silcox, J.; Dellby, N.; Krivanek, O. L. *Science* **2008**, *319*, 1073.

(13) (a) Karlberg, G. S. *Phys. Rev. B* **2006**, *74*, 153414. (b) Stamenkovic, V. R.; Mun, B. S.; Mayrhofer, K. J. J.; Ross, P. N.; Markovic, N. M. *J. Am. Chem. Soc.* **2006**, *128*, 8813. (c) Hammer, B.; Nørskov, J. K. *Adv. Catal.* **2000**, *45*, 71.

JA107874U